Calculations of accommodation coefficients for diatomic molecular gases

Hailemariam Ambaye and J. R. Manson
Department of Physics and Astronomy, Clemson University, Clemson, South Carolina 29634, USA
(Received 14 August 2005; published 27 March 2006)

A theoretical study of energy and momentum accommodation coefficients and reduced force coefficients for molecular gases exchanging energy with surfaces has been carried out. The theoretical model uses classical mechanics for describing translational and rotational motions while internal molecular vibrational modes are treated quantum mechanically. Calculations for diatomic molecular gases are compared with recent measurements using hypersonic beams of N_2 incident on SiO_2 layers deposited on Kapton substrates. The theory gives good qualitative predictions of the behavior of the various accommodation coefficients as functions of the available experimentally controllable parameters such as incident translational energy, incident beam angle, molecular and surface masses, and surface temperature. Quantitative comparisons with measurements for energy and normal momentum accommodation indicate that these experiments can be used to obtain basic physical information about the molecule-surface interaction such as the physisorption potential well depth and the extent of surface roughness.

DOI: 10.1103/PhysRevE.73.031202 PACS number(s): 51.10.+y, 47.40.Ki, 34.50.Dy, 34.50.Pi

I. INTRODUCTION

The concept of thermal accommodation at a gas-surface interface was first introduced by Maxwell [1], who defined the accommodation coefficient as that fraction of particles initially incident on a surface that eventually leaves in equilibrium with the surface temperature. For the energy transfer of a gas of monatomic particles in contact with a surface, a clear definition of the energy accommodation coefficient was later provided by Knudsen who gave a rigorous theoretical foundation for describing it [2–4]. The distribution of the incident gas can take on a range of forms, including such possibilities as a well-defined, monoenergetic incident beam or an equilibrium distribution at a temperature different from that of the surface [5–9].

Although originally defined for the transfer of energy, the methods used to characterize the energy accommodation coefficient have also been extended to describe momentum transfer. The directionality of the momentum transfer is handled by defining momentum accommodation coefficients in mutually perpendicular directions, such as parallel and perpendicular to the surface, or parallel and transverse with respect to the direction of the incident beam of gas [5,10]. Knowledge of the energy and momentum accommodation coefficients is essential for many gas-surface applications such as the rarefied gas dynamics environment of a space vehicle encountering a planetary atmosphere or the energy exchange in gas turbines [5].

Much of the work that has been done on accommodation coefficients, both experimental and theoretical, has been carried out for monatomic gases for which the only energy that is exchanged with the surface by the gas particles is kinetic, or translational. Far less work has been done for molecular gases which have two additional internal degrees of freedom that can transfer energy upon collision with the surface, rotational motion and internal vibrational mode excitation [11,12]. The objective of this paper is to carry out calculations of the accommodation coefficients for diatomic molecular gases using an established theory that has exhibited a demonstrated ability to explain a variety of state-to-state molecule-surface scattering measurements [13–15].

A major motivation for this paper is the availability of recent, high-quality measurements of a variety of accommodation coefficients for several gas-surface systems involving diatomic gases [16–20]. These experiments were all carried out with nearly monoenergetic hyperthermal incident beams of molecular gases such as N_2, O_2, and H_2 under ultrahigh vacuum conditions. The surfaces considered were a variety of clean and adsorbate substrates of technological interest. The best characterized system, and the one to be considered here uses hypersonic jet beams of N_2 incident on a SiO_2-covered Kapton substrate [21].

For the theory used here to interpret the experimental data the translational and rotational motions of the gas molecules are treated classically, but the internal vibrational excitation is treated with quantum mechanics in the semiclassical limit [22,23]. This theory has been applied by the authors to a variety of state-to-state molecule-surface scattering experiments and has been shown to be capable of providing accurate descriptions of the observed scattered angular distributions [15], the translationally energy-resolved intensity spectra [13,14,24], rotational excitation [25], and the internal vibrational mode excitation probabilities [23,25]. Because this theory has successfully demonstrated an ability to explain detailed state-to-state molecular scattering measurements, it is expected that it should also be able to explain the much more averaged energy transfer and momentum transfer measurements that are embodied in the accommodation coefficients. In fact, the accommodation coefficient measurements are of limited content not only because they express integrated averages over the angular and energy distributions of the scattered gas molecules, but also because they do not explicitly measure the internal molecular degrees of freedom and hence do not directly measure energy exchange with the internal modes. Thus a theory that gives a good description of state-to-state measurements should be expected to also give an adequate representation of the behavior of the much more highly averaged accommodation coefficients. In fact,

this is what is found. The calculations presented here provide a quantitative description for the energy accommodation coefficients and normal momentum coefficients measured as functions of the incident angle. Further calculations with the theory provide predictions of the behavior of these coefficients as functions of the other experimentally controllable parameters such as incident translational energy and surface temperature.

In the case of transverse momentum accommodation coefficients the theory underestimates the amount of momentum transferred parallel to the surface. This disagreement is not unexpected since the theory assumes that the repulsive part of the molecule-surface potential is flat except for thermal vibrations, but actual surface conditions may be quite different. Not only will the surface potential appear corrugated at the atomic level, but steps and other types of disorder inherent in real surfaces will considerably enhance the average transfer of momentum parallel to the surface. These types of roughness would, however, have significantly less effect on energy and normal momentum transfer. Thus the disagreement between the present calculations and the measurements for parallel momentum transfer provide a method for estimating the degree of roughness of the surface.

The organization of this paper is as follows: the next section, Sec. II, defines the various accommodation and force coefficients to be considered, Sec. III describes the theory and how it is applied to calculations of the coefficients. Section IV presents the calculated results and comparisons with experiment, and some conclusions are drawn in Sec. V.

II. ACCOMMODATION COEFFICIENTS

The energy accommodation coefficient α_E is normally defined as [4]

$$\alpha_E = \frac{\overline{E}_f^T - \overline{E}_i^T}{\langle E_f^T \rangle - \overline{E}_i^T}, \tag{1}$$

where $\overline{E}_i^T$ is the average translational kinetic energy of a gas molecule in the distribution incident on the surface, $\overline{E}_f^T$ is the average translational energy of the molecules scattered from the surface, and $\langle E_f^T \rangle = 2k_B T_S$, with k_B the Boltzmann constant, is the average translational energy of a molecule leaving the surface in a gas at equilibrium with the same temperature T_S as the surface. For measurements having a well-defined incident beam energy, such as is the case here, $\overline{E}_i^T$ becomes simply the incident kinetic energy E_i^T.

The energy accommodation coefficient as defined in Eq. (1) has a potentially serious flaw because conditions can exist for which the denominator becomes zero and hence α_E becomes singular. This singular behavior becomes a problem only if the incident energy is approximately equal to the average energy $2k_B T_S$. For incident energies much smaller or much larger than $2k_B T_S$, as is almost always the case in this study, the above definition provides a satisfactory representation of the energy transfer.

For situations in which the initial state molecules are in an equilibrium distribution at a gas temperature T_G, the singularity can be avoided by further defining what is known as the equilibrium energy accommodation coefficient. This assumes an equilibrium incident gas and is equivalent to Eq. (1) with $\overline{E}_i^T$ replaced by $\langle E_i^T \rangle = 2k_B T_G$, and then the limit is taken in which the gas and surface temperatures become the same, i.e., $T_G \to T_S$. Defined in this manner, the equilibrium accommodation coefficient is thermodynamically constrained to have values ranging from zero to unity; a value of zero signifying on average elastic scattering with no net exchange of energy between the gas and surface, and a value of unity implying that the gas comes into equilibrium with the surface after collision. Although it is this equilibrium energy accommodation coefficient that is usually treated theoretically, that is not the case here because we wish to analyze experimental data for which the incident gas distribution is a well defined and nearly monoenergetic beam.

Thus a calculation of the energy accommodation coefficient of Eq. (1) becomes a problem of determining the average final energy $\overline{E}_f^T$ which can be calculated from the distribution function of the scattered particles. In the approach used here, this average is obtained from the differential reflection coefficient

$$\frac{dR(\mathbf{p_f}, \mathbf{l_f}, \nu_{jf}; \mathbf{p_i}, \mathbf{l_i}, \nu_{ji})}{dE_f^T d\Omega}. \tag{2}$$

For a molecule initially directed at the surface with linear momentum $\mathbf{p_i}$, angular momentum $\mathbf{l_i}$, and excitation quantum number ν_{ji} where j labels the internal vibration modes, the differential reflection coefficient Eq. (2) gives the state-to-state transition probability in terms of the fraction of incident molecules that are scattered into the energy interval dE_f^T and into the small solid angle $d\Omega$. In experimental terms, dE_f^T can be considered to be the smallest energy interval that can be resolved with the detector and $d\Omega$ is the solid angle subtended by the detector.

Equation (2) gives the state-to-state transition probability, but in the accommodation experiments of interest here, only translational energy exchanges were measured. Thus Eq. (2) must be averaged or summed over all quantities not directly measured. This means that it must be averaged over incident angular momentum and summed over all final angular momentum. For the average over incident angular momenta, we assume that the incident beam has a Maxwell-Boltzmann equilibrium distribution of rotational energies. Similarly, the initial excitation states of the internal molecular modes are averaged and have a Bose-Einstein distribution probability and all final vibrational states are summed for all modes. Finally, since the rotational motion is considered to be classical, the incident molecules can strike the surface at all orientations, so an average over all possible initial orientations is carried out. This averaging and summation process results in a differential reflection coefficient that depends only on the initial and final linear momenta, $dR(\mathbf{p_f}, \mathbf{p_i})/dE_f^T d\Omega$, but still satisfies the condition of unitarity, i.e., it is normalized:

$$\int dE_f^T \int d\Omega \frac{dR(\mathbf{p_f}, \mathbf{p_i})}{dE_f^T d\Omega} = 1. \tag{3}$$

The average final energy needed for Eq. (1) is then given by

$$\overline{E_f^T} = \int dE_f^T \int d\Omega E_f^T \frac{dR(\mathbf{p_f}, \mathbf{p_i})}{dE_f^T d\Omega}. \tag{4}$$

In addition to the energy accommodation coefficient, we will consider here several other types of accommodation involving momentum. The first of these is the pair called the normal (or perpendicular) and transverse (or parallel) momentum accommodation coefficients, $\sigma_\perp$ and $\sigma_\parallel$, respectively. These are given by

$$\sigma_\perp = \frac{\overline{p_{fz}} - \overline{p_{iz}}}{\langle p_{fz} \rangle - \overline{p_{iz}}}, \tag{5}$$

and

$$\sigma = \frac{\overline{P_f} - \overline{P_i}}{\overline{P_i}}, \tag{6}$$

where the momentum is resolved into components parallel and perpendicular to the surface according to $\mathbf{p_f} = (\mathbf{P_f}, p_{fz})$, and in Eq. (6) it is assumed that the quantity P_f or P_i is the respective component of the parallel momentum $\mathbf{P_f}$ or $\mathbf{P_i}$ in the scattering plane (the plane that includes the incident beam and the surface normal direction). For measurements with a beam of well-defined incident momentum, such as considered here, then $\overline{p_{iz}} = p_{iz}$ and $\overline{P_i} = P_i$.

The equilibrium value for the final normal momentum is $\langle p_{fz} \rangle = \sqrt{\pi m k_B T_S / 2}$, where m is the mass of the gas molecule. Clearly, $\langle P_f \rangle = 0$. The averaged final scattered momenta $\overline{P_f}$ and $\overline{p_{fz}}$ are obtained from weighted integrals over the differential reflection coefficient, similar to that for the average translational energy in Eq. (4). In addition to Eqs. (5) and (6) one could define a similar momentum coefficient for the component of parallel momentum perpendicular to the plane of incidence. However, this could be nonzero only for nonisotropic surfaces in nonsymmetry directions and furthermore, measurements of such a quantity have never been reported so it is not considered here.

Also of interest is the scalar momentum accommodation coefficient defined by [19]

$$\mu = \frac{|\overline{\mathbf{p}_f}| - |\overline{\mathbf{p}_i}|}{|\langle \mathbf{p}_f \rangle| - |\overline{\mathbf{p}_i}|}, \tag{7}$$

where $|\langle \mathbf{p}_f \rangle| = \langle p_{fz} \rangle$ is the magnitude of the average momentum of a gas assumed escaping from a surface with complete thermal accommodation [26].

Much of the experimental data discussed in this paper are concerned with an energy accommodation coefficient, somewhat different than that of Eq. (1), which is based on average momentum magnitudes rather than on average energies. This is defined as [19,26]

$$\epsilon_E' = \frac{|\overline{\mathbf{p}_f}|^2 - |\overline{\mathbf{p}_i}|^2}{|\langle \mathbf{p}_f \rangle|^2 - |\overline{\mathbf{p}_i}|^2}. \tag{8}$$

Clearly, the perpendicular momentum accommodation coefficient, the scalar momentum accommodation coefficient, and the energy accommodation coefficients suffer from the same fault, they can have a singularity for particular conditions of surface temperature and incident momentum that can cause their denominators to vanish while the numerators are nonvanishing.

A straightforward solution for avoiding the singular behavior in the momentum coefficients of Eqs. (5) and (6) is to simply normalize the corresponding momentum transfers to the total incident momentum. The standard way of doing this is to define the normal force constant C_n and the tangential force constant C_t as [10]

$$C_n = 2\cos(\theta_i) \frac{\overline{p_{iz}} + \overline{p_{fz}}}{|\overline{\mathbf{p}_i}|}, \tag{9}$$

and

$$C_t = 2\cos(\theta_i) \frac{\overline{P_i} - \overline{P_f}}{|\overline{\mathbf{p}_i}|}, \tag{10}$$

where the factor of $\cos(\theta_i)$ arises because these two coefficients are simultaneously normalized with respect to the area of the incident beam spot on the surface, which increases inversely with the cosine of the polar angle of incidence. Some of the experimental work discussed here is reported in terms of related coefficients which do not contain the $\cos(\theta_i)$ factor, called the perpendicular reduced force coefficient F_z and the parallel reduced force coefficient $F_\parallel$ given by [19,21]

$$F_z = \frac{C_n}{2\cos(\theta_i)}, \tag{11}$$

and

$$F = \frac{C_t}{2\cos(\theta_i)}. \tag{12}$$

These coefficients have two interesting limiting values that can be used as references. If the beam scatters purely elastically from the surface the perpendicular reduced force coefficient becomes $F_z = 2\cos(\theta_i)$ and the parallel reduced force has a value of zero, irrespective of gas or surface species. If the incident beam arrives at thermal equilibrium with the surface upon collision then $F_z = \cos(\theta_i) + \sqrt{\pi m k_B T_S / 2}/p_i$ and $F_\parallel = \sin(\theta_i)$.

III. THEORETICAL MODEL

The above section shows that the accommodation coefficients can be developed in terms of a differential reflection coefficient, which is the quantity that contains all of the information on the gas-surface interaction. The differential reflection coefficient is, in turn, related to the transition rate $w(\mathbf{p}_f, \mathbf{p}_i)$ for making a transition from the initial translational state denoted by momentum $\mathbf{p}_i$ to the state $\mathbf{p}_f$ according to

$$\frac{dR(\mathbf{p}_f, \mathbf{p}_i)}{d\Omega_f dE_f^T} = \frac{1}{2\pi\hbar^3} \frac{m^2 v |\mathbf{p}_f|}{p_{iz}} w(\mathbf{p}_f, \mathbf{p}_i). \tag{13}$$

A classical mechanical expression for describing the state-to-state collisions of atomic gas particles is the differential reflection coefficient for scattering from a smooth surface that has vibrational corrugations due to the motions of the underlying substrate atoms [27–29]:

$$w(\mathbf{p}_f,\mathbf{p}_i)=\frac{2\hbar v_R^2}{S_{uc}}|\tau_{fi}|^2\left(\frac{\pi}{k_BT_S\Delta E_0^T}\right)^{3/2}\times\exp\left(-\frac{(E_f^T-E_i^T+\Delta E_0^T)^2+2v_R^2P^2}{4k_BT_S\Delta E_0^T}\right), \quad (14)$$

where $\Delta E_0^T=\mathbf{p}^2/2M_C$ is the translational recoil energy with $\mathbf{p}=\mathbf{p}_f-\mathbf{p}_i$, M_C is the mass of a substrate atom, $\mathbf{P}$ is the component of $\mathbf{p}$ parallel to the surface, $|\tau_{fi}|^2$ is the scattering form factor, S_{uc} is the area of a unit cell of the substrate, and v_R is a weighted average of phonon speeds parallel to the surface. A calculation of v_R requires knowledge of the surface vibrational spectrum at the position of the classical scattering turning point and is usually treated as a parameter [27,28], although its value should be of the same order of magnitude as the Rayleigh phonon speed.

For the collision of a molecule with a similar smooth vibrating surface, Eq. (14) can be extended to include rotational and vibrational internal modes [22,23]. If the rotational motion is treated classically while the internal vibrational modes are treated with quantum mechanics in the semiclassical limit, the result is

$$w(\mathbf{p}_f,\mathbf{l}_f,\mathbf{p}_i,\mathbf{l}_i)=\frac{\hbar^2}{S_{uc}}|\tau_{fi}|^2\left(\frac{2\pi v_R^2}{\Delta E_0^T k_BT_S}\right)\left(\frac{2\pi\omega_R^2}{\Delta E_0^R k_BT_S}\right)^{1/2}\left(\frac{\pi}{(\Delta E_0^T+\Delta E_0^R)k_BT_S}\right)^{1/2}\exp\left(-\frac{2\mathbf{P}^2v_R^2}{4\Delta E_0^T k_BT_S}\right)\exp\left(-\frac{2l_z^2\omega_R^2}{4\Delta E_0^R k_BT_S}\right)$$
$$\times\sum_{\kappa,\kappa'=1}^{N_A}\left[\cos[(\mathbf{p}_f\cdot\Delta\mathbf{r}_{\kappa,\kappa'}^f-\mathbf{p}_i\cdot\Delta\mathbf{r}_{\kappa,\kappa'}^i)/\hbar\,]e^{-W_\kappa(\mathbf{p}_f,\mathbf{p}_i)}e^{-W_{\kappa'}(\mathbf{p}_f,\mathbf{p}_i)}\prod_{j=1}^{N_\nu}\sum_{\nu_j=-\infty}^{\infty}I_{|\nu_j|}(b_{\kappa,\kappa'}(\omega_j))\left(\frac{n(\omega_j)+1}{n(\omega_j)}\right)^{\nu_j/2}\right.$$
$$\left.\times\exp\left(-\frac{(E_f^T-E_i^T+E_f^R-E_i^R+\Delta E_0^T+\Delta E_0^R+\hbar\sum_{s=1}^{N_\nu}\nu_s\omega_s)^2}{4(\Delta E_0^T+\Delta E_0^R)k_BT_S}\right)\right], \quad (15)$$

where $\mathbf{l}=\mathbf{l}_f-\mathbf{l}_i$, E_i^R and E_f^R are the initial and final rotational energies, the rotational recoil energy is $\Delta E_0^R=l_x^2/2I_{xx}+l_y^2/2I_{yy}+l_z^2/2I_{zz}$ in which the $I_{xx,yy,zz}$ are the principal moments of inertia of the surface. N_A is the number of atoms in the gas molecule with each atom denoted by κ and the number of internal vibrational modes is N_ν. The phase factors in the cosine function arise from quantum-mechanical interference in the excitation of internal vibrational modes and the $\exp\{-W\}$ are the Debye-Waller factors arising from internal vibrational modes. Equation (15) is expressed in a form that is already averaged over a Boltzmann distribution of internal vibrational states whose Bose-Einstein distribution function is $n(\omega_j)$ for the frequency ω_j of the jth mode. The relative strength of each internal vibrational mode is governed by the modified Bessel function I_{ν_j}whose argument is given by

$$b_{\kappa,\kappa'}(\omega_j)=\sum_{\gamma,\gamma'=1}^{3}p_\gamma p_{\gamma'}\frac{1}{N_\nu\hbar\sqrt{m_\kappa m_{\kappa'}}\omega_j}\times e\left(\begin{matrix}\kappa\\ j\end{matrix}\middle|\,\gamma\right)e^*\left(\begin{matrix}\kappa'\\ j\end{matrix}\middle|\,\gamma'\right)\sqrt{n(\omega_j)[n(\omega_j)+1]}, \quad (16)$$

where the $e\left(\begin{matrix}\kappa\\ j\end{matrix}\middle|\,\gamma\right)$ are the γth Cartesian component of the polarization vectors of the κth atom in the jth mode and are determined through a normal-mode analysis of the molecular vibrations. The quantity ω_R is a weighted average of parallel surface librational frequencies. As is the case of the constant v_R, it can be calculated but in this paper it is of no practical importance because we take its value to be so small that it has no detectable effect on the calculated results.

The form factor $|\tau_{fi}|^2$ is determined by the interaction potential. The form factor we use here is one that has proven to be useful in calculating state-to-state scattering probabilities for both atomic and molecular projectiles. This is the Born approximation transition matrix element for scattering by a potential whose repulsive part is exponential, examples being the Jackson-Mott matrix element for a repulsive exponential potential or a Morse potential [30]. In the limit of a very hard repulsive surface, all such matrix elements take on the same form [30], namely

$$|\tau_{fi}|\to|v_{J-M}(p_{fz},p_{iz})|\to 2p_{fz}p_{iz}/m. \quad (17)$$

It is the hard surface limit of Eq. (17) that is used for the form factor in the calculations reported here.

An important aspect in our description of the accommodation process is to address the question of the importance of a precursor physisorption well in the interaction potential. For describing the attractive physisorption well, we choose a square well of depth D. The width of the well is unimportant as long as it is larger than the selvedge region of the surface containing the vibrational amplitudes. Although this may appear to be an overly simple model, for classical translational motion it is a satisfactory choice because it gives the correct acceleration and refraction of the incident particle as it enters the attractive well. Under classical conditions, the principle effects of an attractive adsorption well are to increase the translational energy and to refract the particle so that it collides with the surface at a smaller angle with respect to the normal. A square well includes these two effects in the following way: when the particle enters the well in front of the surface the translational energy in the differential reflection coefficient of Eqs. (13) and (15) is replaced by $E'_{f,i}=E_{f,i}+|D|$, and this increase in energy appears entirely in the nor-

mal momentum according to $p_{iz}'^2 = p_{iz}^2 + 2m|D|$ with a similar expression for p_{fz}'. The differential reflection coefficient inside the attractive well is related to that outside by a simple Jacobian depending on energy, polar angle, and the well depth D.

IV. COMPARISON OF CALCULATIONS WITH MEASUREMENTS

An extensive series of calculations for all of the gas-surface coefficients discussed above in Sec. II has been carried out using the scattering model of Eq. (15). This has allowed us to evaluate the behavior of the theoretical results as functions of the experimentally controllable parameters such as surface temperature, incident beam energy, mass ratio of gas molecule to that of the surface, incident angle, and molecular species.

The results of these calculations will be discussed in the context of comparisons with a recent collection of measurements of many of the different possible accommodation and force coefficients [18–21]. The measurements were made with an experimental apparatus that was capable of directing a hypersonic, well collimated, nearly monoenergetic molecular jet beam with a high flow rate onto a variety of prepared surfaces. Both the transverse and normal force exerted on the sample were measurable. The gases were H_2, N_2, CO, and CO_2 and the surfaces included a variety of materials of practical importance in the manufacture of solar panel arrays, high altitude aircraft, and space vehicles [20]. One of these surfaces was a thick layer of SiO_2 deposited on a Kapton substrate, and that is the system for which we will make all of our comparisons.

The surface of interest can be considered to be amorphous SiO_2, essentially a glass surface, and is well suited for the application of the theoretical model of Eq. (15). The surface is an insulator, and consequently there are no low-energy electron-hole pair excitations expected and the energy transfer will be primarily through multiphonon excitation of the low-energy vibrational modes. At the molecular translational energies of interest, essentially ranging from about 0.5 eV up to 5 eV, the collision will be very much in the classical mechanical regime and the lack of crystal ordering of the amorphous surface will be of no importance.

As stated above in Sec. II the theoretical differential reflection coefficients must be averaged over initial states of the internal molecular modes which are not measured. It is known that supersonic molecular jet sources of the type used in the experiments of interest here produce beams that are rotationally and vibrationally cold, and thus the excitation state distributions for the internal modes can be approximated by equilibrium functions. In the calculations presented here we have carried out the averages assuming that the incident beam rotational and vibrational state distributions are Maxwell-Boltzmann functions with a rotational temperature of 35 K and a vibrational temperatures of 130 K, although the results are essentially independent of these choices as long as they are no larger than room temperature.

In all calculations in this paper the surface mass is taken to be that of a single SiO_2 molecule and the parallel velocity constant is $v_R = 1000$ m/s. There exist no state-to-state measurements for N_2 scattering from SiO_2 that would allow independent determination of the values of these constants through direct comparison of calculated differential reflection coefficients with experimental intensities. However, there are state-to-state scattering measurements for other systems of molecules scattering from insulator surfaces such as C_2H_2/Lif(001) [22,23] and CH_4/LiF(001) [14] and we choose values of mass and v_R consistent with the ones determined for those systems. The dependence of the results on the choice of v_R is very weak for such small values of the order of 1000 m/s used here. If the surface mass is increased the average energy transfer per collision is decreased roughly in accordance with the predictions of the Baule formula, i.e., according to the simple predictions of energy transfer as a function of mass ratio in two-body collisions.

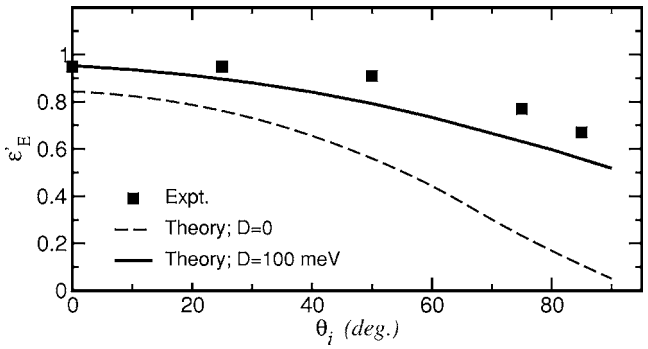

FIG. 1. Energy accommodation coefficient ϵ' as a function of incident angle for N_2/SiO_2. The surface temperature is $T_S = 300$ K and the incident energy is $E_i = 1.47$ eV. The solid curve is theory with well depth $D = 100$ meV, the dashed curve is theory with $D = 0$ and the symbols are experimental data [21,31].

A. Energy accommodation coefficient

Figure 1 shows measurements compared with calculations for the values of the alternate energy accommodation coefficient ϵ_E' as a function of incident angle for the case of an N_2 gas beam incident on a SiO_2 surface. The incident angle is measured with respect to the surface normal, the surface temperature is $T_S = 300$ K, and the beam energy is 1.47 eV which corresponds to an average velocity of 3180 m/s. The measurements [21] are shown as data points [31] and the calculations appear as smooth curves.

The measurements show a value of ϵ_E' slightly less than unity for angles near normal, rising slightly with a weak maximum in the vicinity of $\theta_i = 20°$, but still remaining relatively unchanged up to more than 45° away from normal. At angles larger than 45° the measured values decrease monotonically. Two theoretical curves are shown, the dashed curve is for an interaction potential that has no physisorption well and the solid curve is for an interaction with a potential well depth of 100 meV. The calculations show a monotonically decreasing behavior with increasing incidence angle, slowly decreasing for angles smaller than 45° and increasing more rapidly for larger angles, in general qualitative agreement with the experiment. The calculations with a well depth of

100 meV are in much better quantitative agreement with experiment than those without a well, and this together with further comparisons shown below indicates that the well depth for this system may be of order 100 meV. Such a value would be within the expected range [32], although the value of the well depth for this system is unknown.

In the following we discuss the general properties of the accommodation coefficient as revealed by the calculations. We consider only the case of incident beam energies that are large compared to the temperature of the surface measured in units of $k_B T_S$. This is because of the singularity that appears in the energy accommodation coefficient of Eq. (8) when used with a well defined incident beam. Clearly the results shown in Fig. 1, where the singularity would occur for a beam with incident energy of about 50 meV, satisfies these high incident beam conditions.

Calculations reveal that the two energy accommodation coefficients α_E and ϵ'_E are quite similar. For example, under the conditions of Fig. 1 ϵ'_E is about 2% smaller than α_E, and the reason is that the equilibrium energy $\langle E_f^T \rangle = 2k_B T_S$ appearing in the denominator of Eq. (1) for α_E is considerably larger than the corresponding quantity $|\langle \mathbf{p}_f \rangle|^2/2m = \pi k_B T_S/4$ that appears in Eq. (8) for ϵ'_E [33].

As a function of incident angle the behavior of α_E is qualitatively the same as that exhibited in Fig. 1, as long as the incident energy is large compared to the surface temperature. Although the actual value of α_E depends on system parameters such as molecule and surface species, the calculated energy accommodation coefficient decreases monotonically with increasing incidence angle. Further calculations indicate that, for given values of the potential well depth up to several hundred meV, the value of α_E increases with D. For large incident beam energies, calculations of α_E are monotonically increasing as a function of surface temperature with the increase nearly linear in T_S.

Perhaps the simplest parameter to use for comparing systems consisting of different gases and surfaces is the ratio of gas to surface mass, $\mu = m/M_C$. For large incident energies, α_E is monotonically increasing as a function of μ, with a strongly increasing behavior for small μ, while for μ values approaching unity or slightly larger α_E has a tendency to saturate at values relatively close to unity.

As a function of incident energy the situation is somewhat more complex. For incident energies just above the singularity value α_E increases with incident energy. Depending on the mass ratio μ and well depth D, this increasing behavior may continue monotonically or may result in a local maximum at a certain energy after which there is decreasing behavior to an asymptotic saturation value at large incident energy. In all cases, at large incident energy the value of α_E saturates to a value that depends on the other experimentally controllable parameters as discussed above.

The symmetry or asymmetry of the diatomic molecule has little effect in these calculations, as might be expected from a purely classical treatment of the rotational excitation. For example, the calculated differences in accommodation from the same surface for the two gases N_2 and CO, both having essentially the same mass, is negligible.

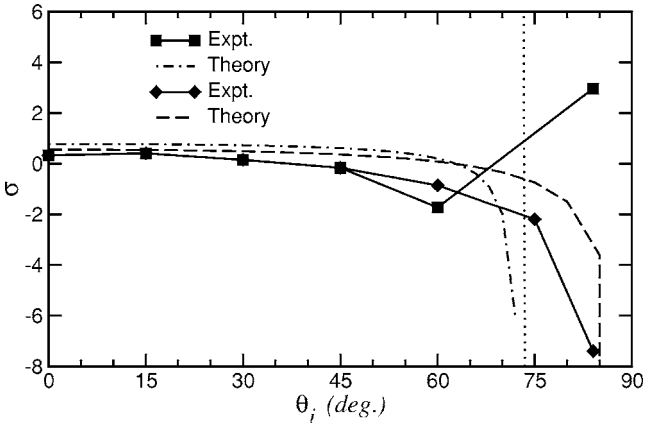

FIG. 2. Normal momentum accommodation coefficient $\sigma_\perp$ as a function of incident angle for N_2/SiO_2 with $T_S = 300$ K and $E_i = 250$ meV. The dash-dotted curve is theory and filled square symbols are experiment [18]. The dashed line is theory and diamond symbols are experiment with $\langle p_{fz} \rangle$ set to zero. The dotted vertical line shows the critical angle $\theta_c = 73.5°$ at which the normal momentum coefficient has its singularity.

B. Momentum accommodation coefficients

We next show some comparisons of the normal, parallel and scalar momentum accommodation coefficients with the available data. Figures 2 and 3 show graphs of the measured and calculated normal momentum accommodation coefficient of Eq. (5) as a function of the angle of incidence. In both figures the surface temperature is 300 K. Figure 2 is for a relatively low incident translational energy of 250 meV where the singularity inherent in the definition of $\sigma_\perp$ is evident at the angle $\theta_i = 73.5°$ and data points [18] appear on both sides of the singularity. The two sets of data shown in Fig. 2 are actually the same, the square points are the momentum coefficient of Eq. (5) (which contains the singularity) and the diamond points are plotted by arbitrarily replacing in Eq. (5) the average normal momentum $\langle p_{fz} \rangle$ by zero, which is a simple way to remove the degeneracy. The corresponding calculations are the dash-dotted and dashed curves,

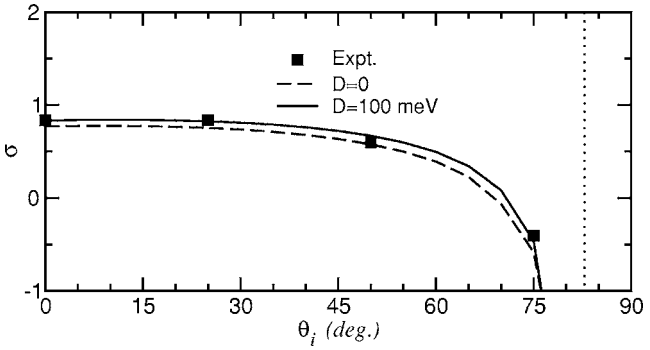

FIG. 3. The normal momentum accommodation coefficient for the same conditions as Fig. 2 except for incident energy $E_i = 1.47$ eV. Two theoretical curves are shown, the solid curve is with well depth $D = 100$ meV dashed curve is with $D = 0$. The dotted vertical line shows the critical angle $\theta_c = 83.3°$ at which the normal momentum coefficient has its singularity.

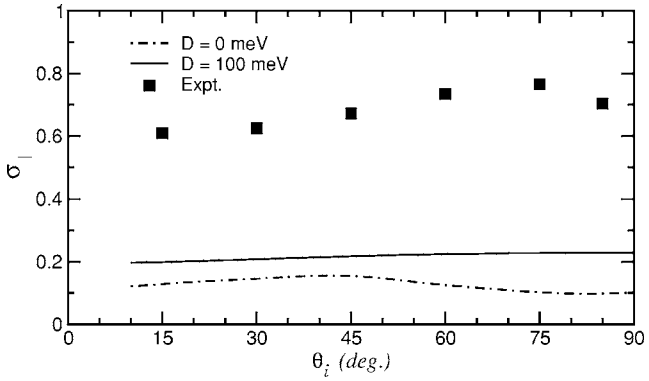

FIG. 4. Incident angle dependence of the parallel momentum accommodation coefficient $\sigma_\parallel$ for the same conditions as in Fig. 2. The solid curve is theory with well depth $D=100$ meV, the dashed curve is theory with $D=0$ and the symbols are experimental data [18].

respectively. The calculations are for $v_R=1000$ m/s and a well depth of $D=100$ meV. Relatively good quantitative agreement is obtained with experiment.

Figure 3 shows the normal momentum accommodation coefficient at the relatively large incident energy $E_i^T=1.47$ eV ($v_i=3180$ m/s). The calculations for both well depths of 0 and 100 meV are shown as solid and dashed curves, respectively. The calculations agree well with the measured experimental points [21], and it is seen that the well has little influence on the calculations when the incident energy is large compared to its depth, as in the case for these conditions.

Figure 4 shows comparisons of calculations with experiment [18] for the parallel momentum accommodation coefficient of Eq. (6) as a function of θ_i for the same low-energy conditions as in Fig. 2. In this case the agreement of calculations with the data is clearly not good, the calculations with or without a physisorption well significantly underestimate the measured parallel momentum exchange. This sort of disagreement with measurements of parallel momentum exchange has been noticed before [34] and is probably due to the fact that the calculations are for a smooth surface whose only corrugations are due to thermal vibrations. However, the real experimental SiO_2 surface is not only corrugated at the atomic level but also contains steps and other large-scale defects, since no special measures were taken to prepare the sample [20], and such defects could greatly enhance the transfer of parallel momentum and thus give enhanced values of $\sigma_\parallel$. This question of the degree of disorder is discussed further in Sec. IV C below in connection with the parallel force coefficient where an estimate of the fraction of the surface covered by defects is obtained.

For the same experimental conditions as in Fig. 1 the scalar momentum coefficient μ of Eq. (7) is shown in Fig. 5. Again, two theoretical calculations are shown for the two well depths of 0 and 100 meV and the experimental data [31] are from Ref. [21]. Interestingly, the same measured and calculated average final momenta are used to determine the energy accommodation coefficient shown in Fig. 1 and for μ, but the agreement between theory and experiment appears

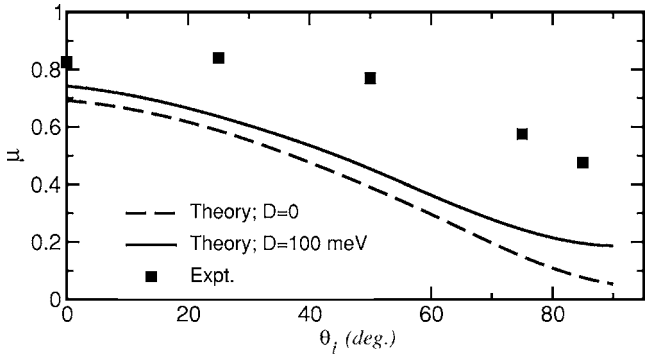

FIG. 5. Scalar momentum accommodation coefficient μ as a function of incident angle for the same conditions as in Fig. 1. The solid line is theory with well depth $D=100$ meV, the dashed line is theory with $D=0$ and symbols are experimental data [21,31].

less good in Fig. 5. This is an illustration of how comparing the same data through differently defined accommodation coefficients can seemingly enhance or decrease the apparent agreement. Thus it is of interest to compare directly the measured and calculated values of the average scattered velocities. Figure 6 shows, again for the same high-energy conditions, the magnitude of the average velocity $|\overline{\mathbf{v}_f}|$ of the gas molecules scattered from the surface as a function of incidence angle. Calculations are compared with the experimental points for the two well depths, and it is seen that the well depth has a significant effect. For zero well depth, the calculations overestimate the average final speed, while for $D=100$ eV the calculated average final speed agrees with the experimental measurement at $\theta_i=0$ and somewhat overestimates it at larger incident angles.

Much better agreement is shown in Fig. 7 which gives the average of the surface-normal component of the final speed as a function of θ_i. The calculations with $D=100$ meV explain the experimental data well. Again, as discussed above in connection with Fig. 1, the better agreement for $D=100$ meV as compared to $D=0$ demonstrates the degree of

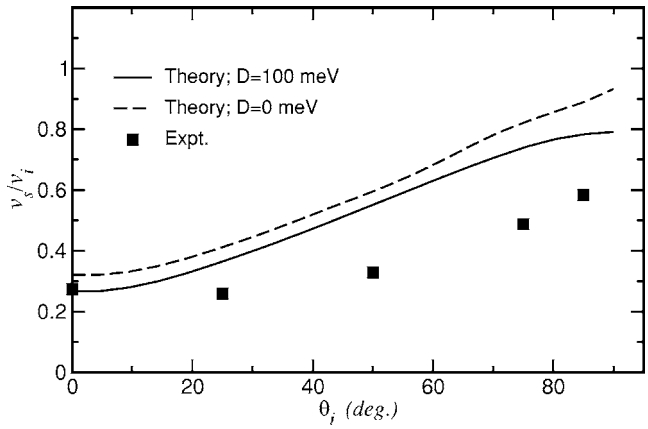

FIG. 6. Experimental values of the normalized final scattering speed [21] v_s/v_i plotted against the incident angle for N_2/SiO_2 for the same conditions as in Fig. 1. The solid curve is the theoretical calculation for $|\overline{\mathbf{v}_f}|/v_i$ with well depth $D=100$ meV, and the dashed curve is for $D=0$.

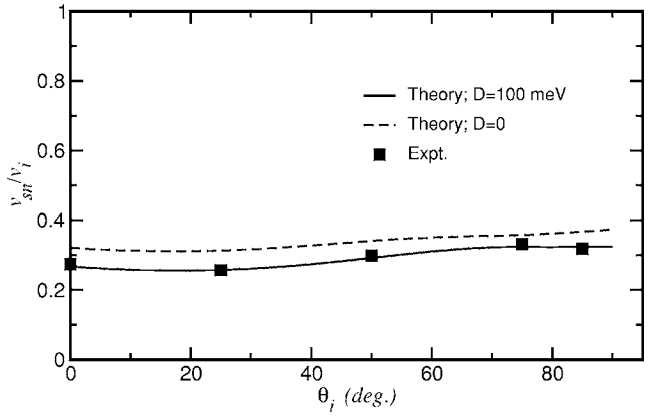

FIG. 7. The measured average scattering speed perpendicular to the surface and normalized by the incident speed v_{sn}/v_i is plotted against the incident angle for N_2/SiO_2 for the same conditions as in Fig. 1 [21]. The solid curve is theory for v_{fz}/v_i with well depth $D=100$ meV and the dashed curve is for $D=0$.

sensitivity of the theory when compared with measurements to determine details of the potential such as the well depth.

C. Force coefficients

The normal and parallel reduced force coefficients plotted as a function of incident angle are shown in Figs. 8 and 9 for the N_2/SiO_2 system with beam energy $E_i=1.47$ eV. As before, the surface temperature is 300 K, and calculations are shown for the two well depths with the parameter $v_R=1000$ m/s. Also shown are curves for the limiting cases of purely elastic scattering and complete thermal accommodation of the beam.

For the case of the normal reduced force coefficient shown in Fig. 8 the measured points decrease from values of approximately 1.3 for normal incidence to a value of about

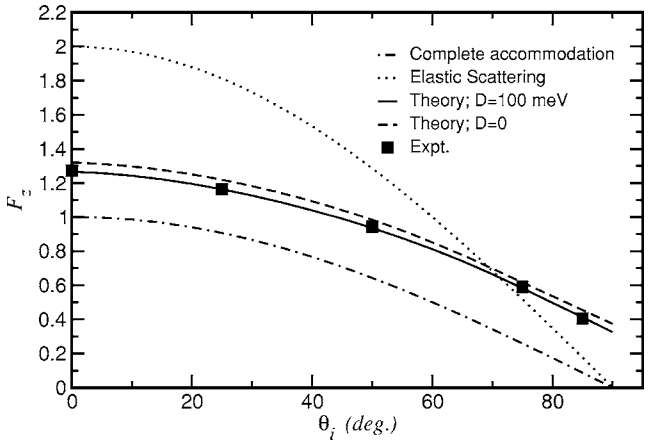

FIG. 8. The normal reduced force coefficient F_z as a function of incident angle for N_2/SiO_2 for the same conditions as in Fig. 1. The solid and dashed curves are calculations with well depths $D=100$ meV and $D=0$, respectively, and the points are the experimental measurements [21]. The dotted curve is the limiting case of elastic scattering and the dash-dotted curve is the limiting case of complete accommodation.

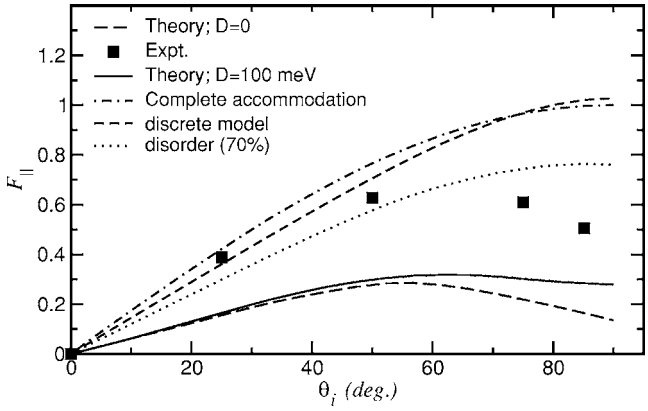

FIG. 9. The parallel reduced force coefficient $F_\parallel$ as a function of incident angle for N_2/SiO_2 for the same conditions as in Fig. 8. The solid and long-dashed curves are calculations with well depths $D=100$ meV and $D=0$, respectively, and the points are the experimental measurements [21]. The dash-dotted curve is the limiting case of complete accommodation and the short-dashed curve is a rough-surface calculation. The dotted curve is the calculation for $D=100$ meV with an estimated 70% of the surface covered with rough disorder.

0.4 at grazing incidence [21]. The measured values disagree quite strongly with the limiting case of elastic scattering, indicating that there is significant energy loss of the incident beam to the surface. However, the experimental points are, for all angles of incidence, larger than the limiting case of an equilibrium final scattering distribution, indicating that the gas molecules do not achieve equilibrium with the surface. The calculated curves agree well quantitatively with the measured points for the normal reduced force coefficient. The calculation for zero well depth somewhat overestimates the measured values by about 10% at small incidence angles, but the calculation for a well depth of 100 meV explains the data quite well.

For the parallel reduced force coefficient shown in Fig. 9, as was the case for the parallel accommodation coefficient of Fig. 4 the calculations agree with the data [21] only qualitatively. Both calculations and measured points increase from a value of zero at normal incidence, reach a maximum between 40° and 60° and then decrease to a nonzero value at grazing incidence. However, the calculated values, regardless of well depth, are significantly smaller than the measurements. The likely explanation for this discrepancy is the same as was given for the parallel momentum coefficient of Fig. 4 above, i.e., the calculations are for a smooth surface while the experimentally measured surface probably had significant roughness that would enhance parallel momentum transfer.

In fact, if it is assumed that the difference between the calculations and experimental data in Fig. 9 is due to surface disorder, that difference provides a way of estimating the fraction of an otherwise smooth surface that can be considered to be disordered. For example, a calculation of the parallel reduced force coefficient for a disordered surface should overestimate the experimental measurements. A useful model that has been used to describe disorder is a surface covered with discrete scattering centers, known as the discrete surface model [27,34]. Equation (14) with v_R set equal to zero,

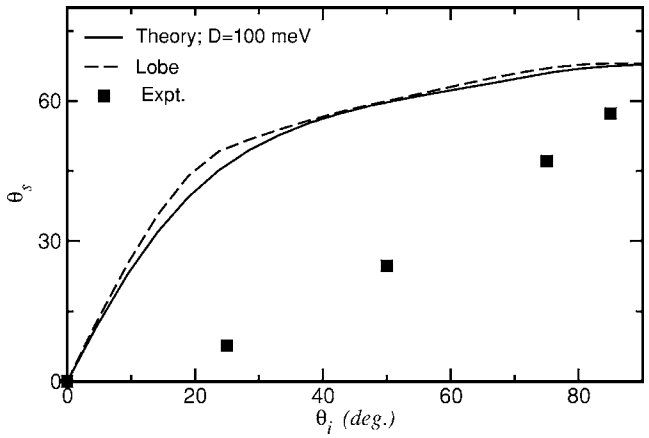

FIG. 10. Final scattered angle θ_s vs incident angle. The measurements [21] are shown as points, the calculations with a well depth $D=100$ meV are the solid line curve, and the dashed curve is the position of the most probable intensity in the calculated angular distribution lobe.

the exponent 3/2 of the prefactor replaced by 1/2 and with a constant scattering form factor $|\tau_{fi}|^2=1$, is a good model for the inelastic scattering of an atomic particle from a surface covered with disorder modeled by hard hemispherical bumps [34]. This rough-surface calculation for pseudoatomic N_2 is shown as the short-dashed curve in Fig. 9. The results are quite close to the curve for the limiting case of complete thermal accommodation, a behavior that is supported by experimental measurements from very rough surfaces that produce parallel force coefficients very close to the thermal accommodation limit [20]. Thus if the experimental data can be matched by adding a fraction of the value calculated for a disordered surface to the theoretical calculations of N_2 scattering from a smooth surface, that fraction would be equivalent to the effective fraction of the surface covered by disorder. Such a calculation is shown in Fig. 9 by the dotted curve, which is the sum of 0.70 times the rough surface value of $F_\parallel$ (short-dashed curve) plus 0.3 times the value calculated for $D=100$ meV (solid curve). This, then, gives a crude estimate of the percentage of an otherwise smooth surface that can be considered to be covered by disorder. It indicates that the experimental data can be crudely matched by scattering from an otherwise flat surface that has 70% of its area covered by roughness.

D. Average scattering angle

The measured and calculated average final scattering angles are shown in Fig. 10. The experimental points were obtained from the relation

$$\theta_s = \tan^{-1}(v_{st}/v_{sn}), \tag{18}$$

where v_{st} and v_{sn} are the measured average speeds parallel and perpendicular to the surface, respectively. The calculated values are shown by the solid curve. The disagreement exhibited in Fig. 10 between the calculated θ_s and the measurements for non-normal incident angles is due to the fact that the theory produces a value of the final average speed parallel to the surface that is larger than the measured values. Also shown in Fig. 10 as a dashed curve is the position of the most probable intensity in the scattered angular distribution. The two different calculational methods for defining the average final angle give quite similar results.

However, the calculated values of normal speeds $\overline{v_{fz}}$ shown in Fig. 7 are in very good agreement with measurements. Thus the disagreement with experiment apparent in the average final angles of Fig. 10 is most probably due to surface roughness, as discussed above in connection with the force coefficients in Sec. IV C. For example, the dotted curve in Fig. 9, which assumes a fraction of the surface is covered by disorder, implies a value of the average final parallel speed. If this implied average final parallel speed is used with $\overline{v_{fz}}$ to calculate the average final angle from a tangent relation similar to Eq. (18), the results agree reasonably well with the measurements.

V. DISCUSSION AND CONCLUSIONS

This paper presents the results of calculations of the energy accommodation coefficient for the interaction of a beam of molecular gas with a surface, as well as calculations for several forms of the various types of momentum accommodation coefficients. The calculations are carried out for a diatomic molecular gas, including internal rotational and vibrational degrees of freedom, and the theoretical model for the gas-surface collision interaction is based on fully three-dimensional scattering cross sections. The translational and rotational degrees of freedom are treated with classical mechanics while the internal molecular vibrational modes are calculated quantum mechanically.

These calculations are compared with recent measurements of the energy accommodation coefficient and the momentum accommodation coefficients for well-defined and monoenergetic beams of N_2 gas directed towards a surface of amorphous SiO_2 coating a Kapton substrate [18–21]. Good agreement between theory and experiment is obtained for many of the measurements indicating that the theory is useful in explaining and predicting observed physical results. Although the calculations shown here are limited to those for which the experimental data are available, the theory can be readily extended to other molecules, including multiatomic molecules, and to other surfaces.

Knowledge of accommodation coefficients of various types is extremely important in technological problems involving gas-surface interactions [5,30]. Nevertheless, the general perception appears to be that, since they represent highly averaged quantities in which the complexity of the molecule-surface interaction is reduced to a single parameter, accommodation coefficients are not particularly useful for determining fundamental properties. However, an interesting result to arise from this work is that certain basic, fundamental properties of the gas-surface potential may be extracted from accommodation coefficient measurements. In particular, the comparisons here for the energy accommodation coefficient and particularly for the momentum accommodation coefficients involving normal momentum transfer show better agreement with measured data for an interaction potential

that contains a physisorption well with depth of about 100 meV than for calculations that have no well. Although the potential well depth is not known for the N_2/SiO_2 system, based on knowledge of other systems, a value of that order of magnitude is expected [32].

A second basic property of the scattering system that can be addressed by comparing the present calculations to the experimental data is estimating the extent of surface roughness. One seeming failure of the present calculations involves predictions of measured values of the accommodation and force coefficients for momentum transfer parallel to the surface. Both the parallel momentum accommodation coefficients and the parallel force constants appear to be significantly underestimated by the theory. This is a problem that has been observed previously for other theoretical comparisons with parallel momentum transfer measurements [34]. However, the reason for this discrepancy appears to be understood. The calculations are carried out for a model of the surface that is smooth and flat except for corrugations due to thermal vibrations, i.e., the average surface barrier is assumed to be flat. However, the surfaces used for most measurements, and certainly the amorphous glass surfaces considered here, have a variety of roughness including atomic-scale corrugation, defects and steps. Roughness on the surface, particularly large-scale roughness such as steps, will provide mechanisms for parallel momentum transfer that are not included in the theory. This enhanced parallel momentum transfer would lead to larger parallel momentum coefficient values than would be expected for a surface that is on average flat. Thus through comparison of the present ordered-surface calculations with results expected for scattering from disordered surfaces we have been able to estimate that the effective fraction of the surface area that can be considered rough is about 70%.

As interesting aspect that is emphasized by the present comparison of calculations with experimental measurements is that the several different kinds of accommodation and force coefficients can augment or decrease the apparent discrepancies between calculations and data. In the experiments of interest here [18,20,21], the data obtained consist of measurements of the normal and tangential force constants, which is equivalent to measuring the average final speeds normal and parallel to the surface. Thus the information presented for the energy accommodation coefficient in Fig. 1 and the scalar momentum accommodation coefficient of Fig. 5 are the same. However, the apparent agreement between theory and experiment seems better for the energy accommodation coefficient than for the scalar momentum coefficient.

Perhaps the best way to present the comparison of the measurements with theory is through the direct comparisons of the average final speed shown in Fig. 6 or the average final speed normal to the surface of Fig. 7. Clearly, the theory presented here explains qualitatively the variation of these speeds with incident angle, and the average normal speed is in good quantitative agreement with experiment. (The theory does not give good predictions for the parallel force coefficients, indicating that the average final speed parallel to the surface does not agree with measurements, but as discussed above this is probably due to disorder on the surface.)

One important result of the present work is that the theoretical model is sufficiently sophisticated that it should give a good indication of the effects on the accommodation coefficients of energy transfer to internal molecular modes. The experiments considered here measured only translational kinetic energy and momenta. The internal states of the incident molecular beams were not measured, but it is known that molecular beams from a hypersonic jet source tend to be rotationally and vibrationally cold. Thus if there is significant energy transferred into excitation of internal modes during the collision process this can affect the measured values of the translational accommodation coefficients. The effect, for a rotationally and vibrationally cold incident beam, would be to lower the final average translational energies and momenta because energy would go into the internal modes. Such effects can be directly compared in the current calculation by carrying out calculations in which the molecule is replaced by a pseudoatom having the same mass. In general, it is found that for the range of beam conditions and molecular systems studied here, the effect of the molecular internal modes is relatively small. For example, molecular calculations of the energy accommodation coefficient such as shown in Fig. 1 are about 1% larger than those for the corresponding pseudoatomic gas. Similar changes are found for the case of the perpendicular force coefficients of Fig. 2. Essentially all of this small effect is due to excitation of rotational motion. Although there is some internal mode excitation, at the incident translational energies of order of a few eV considered here the internal mode excitation probability is small and energy transferred to those modes has negligible effect.

An interesting observation concerning the present calculations is that they have the advantage that they are based on differential reflection coefficients for the surface collision that are expressed in analytic forms, namely Eq. (15) for molecular scattering and Eq. (14) for atomic gases. This means that in many cases, without carrying out extensive calculations, it is possible to predict the behavior of accommodation and force coefficients as functions of the experimentally controllable parameters such as beam energy, incidence angle, mass of the gas, mass distribution of the surface, or surface temperature. The theory developed here can readily be extended to situations involving more complex surfaces containing multiple atomic species, such as might be expected in technological applications. It can also be extended to gases containing multiple species. Thus because it is based on analytic forms for the scattering differential reflection coefficients the present theoretical model should be useful for making qualitative predictions, and as evidenced in this work, sometimes quantitative predictions of accommodation coefficient behavior.

ACKNOWLEDGMENTS

This work was supported by the National Science Foundation under Grant No. DMR-0089503 and by the Department of Energy under Grant No. DE-FG02-98ER45704.

[1] J. C. Maxwell, Philos. Trans. R. Soc. London **170**, 251 (1879).
[2] M. Knudsen, Ann. Phys. **48**, 1113 (1915); **28**, 999 (1909).
[3] M. Knudsen, Ann. Phys. **32**, 809 (1910).
[4] M. Knudsen, *The Theory of Gases* (Methuen, London, 1934).
[5] S. C. Saxena and R. K. Joshi, Thermal Accommodation and Adsorption Coefficients of Gases, *CINDAS Data Series on Material Properties*, edited by C. Y. Ho (Hemisphere, New York, 1989).
[6] F. O. Goodman, J. Chem. Phys. **50**, 3855 (1969).
[7] F. O. Goodman, J. Chem. Phys. **56**, 6082 (1972).
[8] J. R. Manson, J. Chem. Phys. **56**, 3451 (1972).
[9] B. Gaffney and J. R. Manson, J. Chem. Phys. **62**, 2508 (1975).
[10] S. A. Schaaf and P. L. Chambré, in *High Speed Aerodynamics and Jet Propulsion*, edited by H. W. Emmons (Princeton University Press, Princeton, NJ, 1958), Vol. 3, Sec. H, pp. 687–739.
[11] G. M. Rosenblatt, R. S. Lemons, and C. W. Draper, J. Chem. Phys. **67**, 1099 (1977).
[12] D. R. Anderson, E.-H. Lee, R. H. Pildes, and S. L. Bernasek, J. Chem. Phys. **75**, 4621 (1981).
[13] I. Iftimia and J. R. Manson, Phys. Rev. B **65**, 125412 (2002).
[14] I. Moroz and J. R. Manson, Phys. Rev. B **69**, 205406 (2004).
[15] H. Ambaye, J. R. Manson, O. Weibe, C. Wesenberg, M. Binetti, and E. Hasselbrink, J. Chem. Phys. **121**, 1901 (2004).
[16] R. H. Krech, M. J. Gauthier, and G. E. Caledonia, J. Spacecr. Rockets **30** (4), 509 (1993).
[17] G. E. Caledonia, R. H. Krech, B. L. Upschulte, K. W. Holtzclaw, and D. B. Oakes, *AIAA–94–2638, Proceedings of the 18th AIAA Aerospace Ground Testing Conference*, Colorado Springs (1994).
[18] S. R. Cook, J. B. Cross, and M. Hoffbauer, *AIAA–94–2637, Proceedings of the 18th Aerospace Ground Testing Conference*, Colorado Springs (1994).
[19] S. R. Cook and M. A. Hoffbauer, Phys. Rev. E **55**, R3828 (1997).
[20] S. R. Cook, M. A. Hoffbauer, D. D. Clark, and J. B. Cross, Phys. Rev. E **58**, 492 (1998).
[21] S. R. Cook and M. A. Hoffbauer, Phys. Rev. E **58**, 504 (1998).
[22] I. Iftimia and J. R. Manson, Phys. Rev. Lett. **87**, 093201 (2001).
[23] I. Iftimia and J. R. Manson, Phys. Rev. B **65**, 125401 (2002).
[24] I. Moroz and J. R. Manson, Phys. Rev. B **71**, 113405 (2005).
[25] H. Ambaye and J. R. Manson (unpublished).
[26] An alternative definition of the scalar momentum accommodation coefficient of Eq. (7) and the energy accommodation coefficient of Eq. (8) could be made based on the average of the magnitude of the momenta, in which case $|\langle \mathbf{p}_f \rangle| = \langle p_{fz} \rangle$ would be replaced by $\langle |\mathbf{p}_f| \rangle = 3\langle p_{fz} \rangle / 2$. However, the definitions appearing in Eqs. (7) and (8) are consistent with the physical quantities actually measured in the experiments [19–21] of interest here.
[27] R. Brako and D. M. Newns, Phys. Rev. Lett. **48**, 1859 (1982).
[28] H. D. Meyer and R. D. Levine, Chem. Phys. **85**, 189 (1984).
[29] J. R. Manson, Phys. Rev. B **43**, 6924 (1991).
[30] F. O. Goodman and H. Y. Wachman, *Dynamics of Gas-Surface Scattering* (Academic Press, New York, 1976).
[31] These data points are taken from Fig. 5 of Ref. [21]. In that figure, which contains data for both the alternate energy accommodation coefficient ϵ_E' and the scalar momentum accommodation coefficient μ, the two curves are mislabeled. The data labeled ϵ_E' should be for μ and vice versa.
[32] G. Vidali, G. Ihm, H.-Y. Kim, and M. W. Cole, Surf. Sci. Rep. **12**, 133 (1991).
[33] If instead, as suggested in Ref. [26] above, an alternatative definition for ϵ_E' based on the average of the magnitude of the momenta is used, then the corresponding effective equilibrium energy $|\langle \mathbf{p}_f \rangle|^2 / 2m = \pi k_B T_S / 4$ in Eq. (8) would be replaced by $\langle |\mathbf{p}_f| \rangle^2 / 2m = 9\pi k_B T_S / 16$ and the difference between the calculations of this version of ϵ_E' and α_E becomes less than one-half of one percent. For comparison, the average energy of a gas particle in an equilibrium Knudsen flux, which appears in the definition of Eq. (1) for α_E is $\langle \mathbf{p}_f^2 \rangle / 2m = 2k_B T_S$.
[34] H. Legge, J. R. Manson, and J. P. Toennies, J. Chem. Phys. **110**, 8767 (1999).